

**Cite this article**

Batagoda JH, Hewage SDA and Meegoda JN  
Remediation of heavy-metal-contaminated sediments in USA using ultrasound and ozone nanobubbles. *Journal of Environmental Engineering and Science*,  
<https://doi.org/10.1680/jenes.18.00012>

**Research Article**

Paper 1800012  
Received 26/04/2018; Accepted 22/01/2019

**Keywords:** environment

ICE Publishing: All rights reserved

# Remediation of heavy-metal-contaminated sediments in USA using ultrasound and ozone nanobubbles

**Janitha Hewa Batagoda** PhD

Adjunct Professor, Department of Civil and Environmental Engineering, New Jersey Institute of Technology, Newark, NJ, USA (corresponding author: [jh358@njit.edu](mailto:jh358@njit.edu)) (Orcid:0000-0003-2616-150X)

**Shaini Dilsha Aluthgun Hewage** MSc

PhD student, Department of Civil and Environmental Engineering, New Jersey Institute of Technology, Newark, NJ, USA (Orcid:0000-0001-7767-0000)

**Jay N. Meegoda** PhD, PE

Professor, Department of Civil and Environmental Engineering, New Jersey Institute of Technology, Newark, NJ, USA (Orcid:0000-0002-8406-7186)

The lower 12.875 km of the Passaic River is heavily contaminated due to industrial activities – specifically heavy metal extraction from chromium-ore-processing plants and production of pesticides and herbicides. Conventional methods for remediating contaminated sediments have limited application due to the tidal action and urban area of the contaminated section of the Passaic River. Hence, this study proposes an in situ technology using ultrasound and ozone nanobubbles to remediate the sediments. Ultrasound is capable of desorbing heavy metals from soil, and ozone can oxidise the released heavy metals to a form that is mobile for ease of extraction. Nanobubbles are used as an effective ozone delivery method for the oxidation of heavy metals. Bench-scale tests were performed to evaluate the feasibility of the proposed technology. Ozone nanobubbles increased the solubility of ozone in water and reduced wastage. Also, due to the high ozone concentrations in water, chromium oxidation increased. A synthetic soil with a grain size distribution similar to that of actual river sediments was artificially contaminated with chromium and used in this research. Test results showed a 97.54% chromium removal efficiency, suggesting the feasibility of the proposed technology for pilot-scale studies.

## Notation

 $E$  removal efficiency $I$  initial chromium concentration in the specimen $O$  chromium concentration at the end of the experiment

action and urban area of the contaminated section of the Passaic River.

This study proposes a coherent and novel remediation technology using ultrasound and ozone ( $O_3$ ) nanobubbles. The conceptual sketch proposed technology is shown in Figure 1. The proposed in situ remediation technology involves a containment chamber being partially lowered into the contaminated sediments, allowing space for ozone-nanobubble-saturated water to be delivered into the chamber. Inside the chamber, ultrasound agitates the contaminated sediments, breaking their absorption bonds and allowing ozone to oxidise the contaminants. The oxidised chromium is water soluble and hence will be in the liquid phase. Therefore, the sediments are allowed to settle and the resulting effluent containing oxidised chromium will be extracted and treated using a nanofiltration system.

This bench-scale study evaluated the proposed technology by investigating the use of ozone nanobubbles and ultrasound to remediate contaminated sediments.

## Ultrasound

The propagation of ultrasound through a liquid promotes four different responses: heating due to the dissipation of acoustic energy, formation of gas/vapour bubbles termed 'cavitation', violent collapse of cavitation generating high shear forces and fluid flow termed 'microstreaming' (Newman *et al.*, 1997).

For decades, the Passaic River was used to transport products from many industries established along the river to Newark Bay Harbor. The navigation channel ranged from 45 to 90 m wide, which was nearly 50% of the total bank-to-bank width of the river (USACE, 1973). Dredging to maintain the navigational channel was stopped in the 1970s due to heavy contamination of the river. Conventional methods for remediating the contaminated sediments have limited application due to the tidal

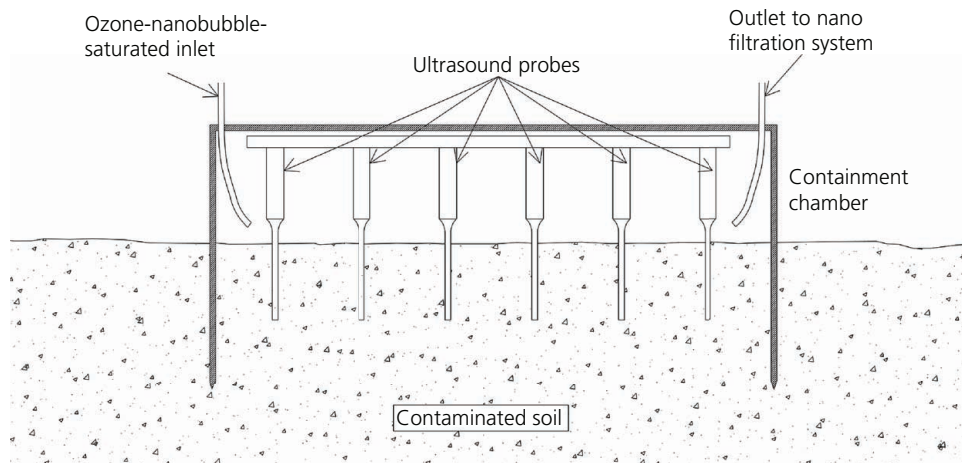


Figure 1. Conceptual sketch of the proposed remediation technology (Meegoda *et al.*, 2017)

These shear forces are capable of removing material adhered to surfaces.

Ultrasound has been the focus of numerous studies. The low-frequency application of ultrasound from 20 to 100 kHz has been used in industrial cleaning, including sediment washing (Meegoda and Perera, 2001; Meegoda and Veerawat, 2002). Soil washing is one of the most common technologies used in ex situ remediation. Many researchers investigated the use of ultrasound to enhance soil washing by replacing mechanical mixing. Bagal and Gogate (2012) investigated the possibility of using ultrasound to remove the herbicide alachlor. They used a 20 kHz ultrasound at 100 W power to remove alachlor at high efficiencies, where the Fenton reaction was used to improve oxidation. Babić *et al.* (1998) examined the efficiency and rate of extraction in ultrasonic solvent extraction, Soxhlet extraction and shake-flask extraction. They found that the rate of solvent extraction using ultrasound was higher than that using shake-flask and Soxhlet extraction. The use of ultrasound to remediate soil contaminated with heavy metals has also been investigated. Kyllonen *et al.* (2004) identified the capability of using ultrasound to process minerals where they used ultrasound to separate lead (Pb) and zinc from soil at the industrial scale. Newman *et al.* (1997) studied the use of ultrasound to remove contaminants from bricks embedded with copper oxide, achieving a 40% reduction of copper oxide, compared to 6% reduction of copper oxide achieved using mechanical mixing.

### Ozone nanobubbles

Ozone is a highly unstable oxidiser used in many industries due to its oxidising capacity and its ability to manufacture on demand. Industries using ozone include cloth manufacturing, waste water treatment, produce preparation and contaminant remediation (Choi *et al.*, 2001; Masten and Davies, 1997; O'Mahony *et al.*, 2006). Several researchers (Do *et al.*, 2009; Li *et al.*, 2014; Yu *et al.*, 2007) investigated the influence of soil grain size on ozonation of

soil contaminated with organics. Leštan and Finžgar (2007) used ozone and UV (ultraviolet) to leach ethylenediaminetetraacetic acid-lead from the soil and showed 58.4% lead removed from the soil. Rodman *et al.* (2006) studied the use of advanced oxidation methods which included ozone to convert chromium (III) propionate to chromium (VI). With advanced oxidation methods, heavy metals are converted to a higher oxidation state, making them highly mobile (O'Mahony *et al.*, 2006) and water soluble and making it possible to separate them by precipitation and filtration (Seo *et al.*, 2010).

However, due to the short half-life of ozone in water, ozone delivery to contaminated sediments using conventional methods is ineffective and wasteful. In order to increase the efficient use of ozone and efficient oxidation of contaminated sediments, this study used ozone-infused nanobubbles to saturate and deliver ozone to contaminated sediments. The prolonged lifespan of ozone-infused nanobubbles helped keep the water saturated with ozone.

Nanobubbles were selected for use in this study due to their longer lifespan in water compared to those of macro- and micro-bubbles. The most likely mechanisms for the prolonged stability of nanobubbles includes hydrogen bonds on the interface of bubbles (Ohgaki *et al.*, 2010), formation of bubble clusters (Bunkin *et al.*, 2012; Jin *et al.*, 2007; Sedlák, 2006a, 2006b), available ions in water (Bunkin *et al.*, 2012; Hampton and Nguyen, 2010) and supersaturated liquid next to the bubble surface (Brenner and Lohse, 2008).

Many researchers have investigated advantages of using nanobubbles in various fields, including medicine (Choi *et al.*, 2001; Modi *et al.*, 2014; Mondal *et al.*, 2012), control of boundary slip (Li *et al.*, 2016; Wang *et al.*, 2009), bioremediation (Li *et al.*, 2014; Pan and Yang, 2012) and water treatment by flotation (Li *et al.*, 2009). Takahashi (2009) proposed the use

of nano-air-bubbles to treat waste water. Khuntia *et al.* (2013) investigated the possibility of using ozone micro- and nano-bubbles to purify drinking water. Ikeura *et al.* (2011) effectively removed fenitrothion from vegetables using micro–nano–ozone bubbles.

## Materials and methods

### Materials

Sediments from the Passaic River are contaminated with a verity of organic and inorganic pollutants, including polycyclic aromatic hydrocarbons, polychlorinated biphenyl, chromium, nickel (Ni), cadmium (Cd) and mercury (Hg). For the purposes of this bench-scale study, a synthetic soil was developed and mixed with one heavy metal (chromium). Only one heavy metal was used in the study, since obtaining and controlling the other pollutants was not a viable option due to cost, regulation of the New Jersey Department of Environmental Protection (NJDEP) and the complication to laboratory experiments due to the variety of pollutants in varying concentrations (Meegoda and Perera, 2001). Also, the authors had extensive experience dealing with chromium. The particle size distribution of the synthesised soil is shown in Figure 2, which closely matches that of sediment samples obtained from the Passaic River. The soil was a mixture of rock flour, kaolin and sand that had a similar size distribution as the river sediments. The synthetic soil also had similar adsorption as that of river sediments (Meegoda and Veerawat, 2002).

### Sample preparation

The chromium (III) compound chromium (III) chloride hexahydrate ( $\text{CrCl}_3 \cdot 6\text{H}_2\text{O}$ ) was used in the study to contaminate the synthetic soil. The study used chromium (III) chloride hexahydrate due to its usability in laboratory settings and its non-toxic nature, which did not require modifications to the lab to

handle the chemical, and because chromium (III) chloride hexahydrate mimics the behaviour of other heavy metals found in Passaic River sediments. To prepare the sample, 1 g of chromium (III) chloride hexahydrate was mixed with 50 ml of deionised (DI) water and was stirred until chromium (III) chloride was dissolved. The resulting liquid was mixed with 80 g of synthetic soil for 1 h using a mechanical mixer. The sample was then placed in an oven for 24 h at a temperature of 40°C to evaporate the excess water. Then, the sample was heated for 3 h in a high-temperature oven at 850°C in an oxygen-less environment to make chromium-contaminated soil with adsorption bonds between chromium and soil particles. The oxygen-less environment was created by injecting nitrogen into the oven to prevent chromium from oxidising during heat treatment. After 3 h, the oven was turned off, yet nitrogen injection continued until the sample reached room temperature.

### Ozone nanobubble generation

Ozone for this research was produced by passing industrial-grade oxygen through an ozonator (A2Z Ozone Inc., model MP-3000). Nanobubbles were generated with a micro–nano–bubble nozzle (model BT-50FR, Riverforest Corporation, USA) where the rotational flow of water in a high-pressure chamber was used to generate nanobubbles. Ozone gas was introduced to the inlet of the utility pump through a nanobubble nozzle (model 4CUK6, Dayton, USA) to produce ozone nanobubbles. The pump generated a constant running pressure of 55 pounds/inch<sup>2</sup> (379 kPa) during operations to optimise the bubble generation. The nanobubble generation system and the components used are shown in Figure 3(a).

### Experimental procedure

A 40 g sample of synthetic soil contaminated with chromium chloride was placed in the reaction chamber (see Figure 3(b)). The sample size was kept at 40 g to reduce the contaminant effluent, which required special disposal to comply with NJDEP regulations. The remediation chamber was made of a high-density polyethylene base and a high-density polycarbonate shell. The soil was placed at the bottom of the chamber and was subjected to varying amounts of ultrasound power and dwell time, ozone-nanobubble-saturated water, temperature and pH values. The water was then drained out of the chamber through a filtering mesh and was collected in a 20 litre container where it was allowed to settle. Water was filtered out from settled soil and returned to the reaction chamber to minimise the soil lost during the experiment.

### Chemical analysis

#### Analysis of heavy metal concentration

The treated contaminated synthetic soil samples were dried at 40°C. A 1.0 g sample was collected from the dried soil and was digested using 10 ml of trace-metal-grade nitric acid (67–70% w/w). Then, the mixture was heated at low temperatures (70–80°C) until the full sample dissolved in nitric acid. The solution was diluted by adding 990 ml of deionised water, bringing the total solution volume to 1000 ml. Then, the diluted nitric acid digested samples were tested

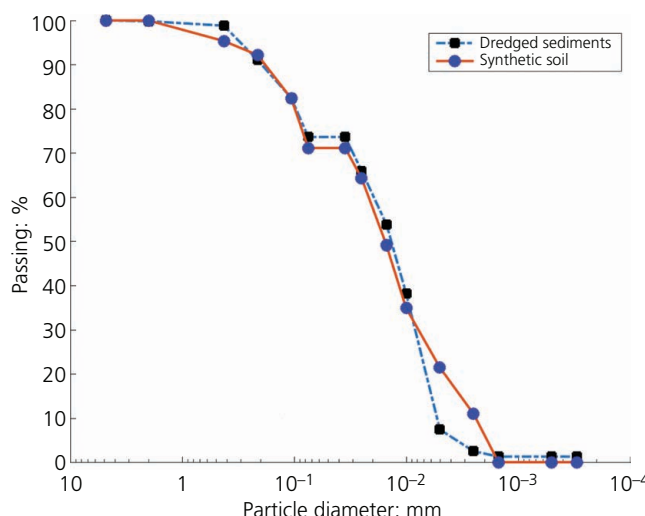


Figure 2. Particle size distributions of the synthetic soil and dredged sediments

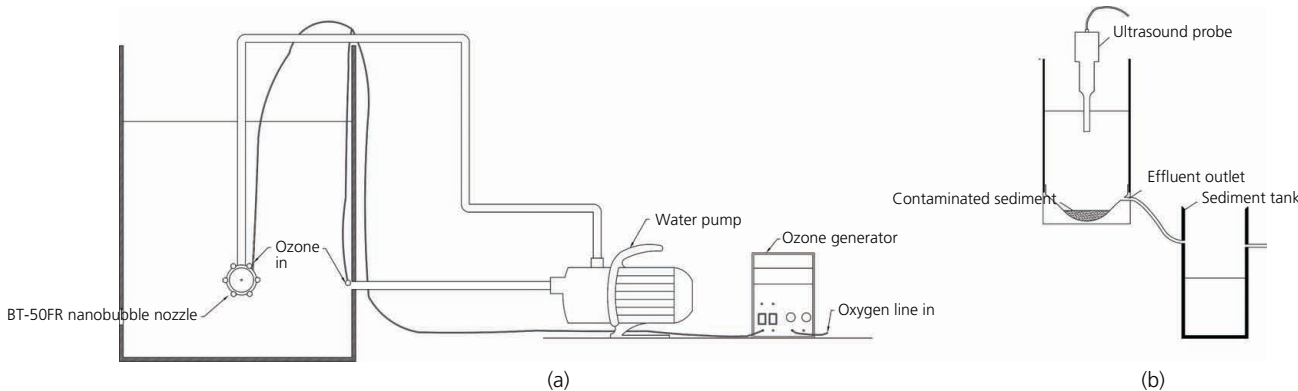


Figure 3. (a) Ozone nanobubble generation system; (b) contaminant remediation set-up

using both atomic absorption spectrometry as well as inductively coupled plasma mass spectrometry to obtain the metal concentration and to identify and control for possible errors due to equipment malfunction.

#### Dissolved ozone analysis

The dissolved ozone was measured using the 4500-O<sub>3</sub> indigo colorimetric method (Rice *et al.*, 2017). A Thermo Scientific 220 UV-visible spectrophotometer was used to evaluate the adsorption of ozone.

#### Dissolved oxygen analysis

Dissolved oxygen levels in water were measured using an Orion Star A329 optical dissolved oxygen and pH monitor. This monitor is capable of measuring oxygen levels in water from 0·00 to 90·00 mg/l with an accuracy of  $\pm 0\cdot 2$  mg/l.

#### Nanobubble analysis

The ozone nanobubbles were tested every ten remediation cycles to determine the bubble size distribution and the zeta potential values of the bubbles to detect variations in bubble generation. A Malvern Zetasizer Nano instrument was used to analyse the bubble size distribution and zeta potential values of nanobubbles. To analyse the bubble size, 12 mm square polystyrene cuvettes was used, and to analyse the zeta potential, a folded capillary zeta cell (model DTS1070) was used.

## Results and discussion

### Ozone nanobubble size distribution and zeta potential

The removal efficiency of chromium-contaminated soil depends on the amount of dissolved ozone in water. The stability of nanobubbles and the zeta potential are two key factors that determined the amount of dissolved ozone in water. Nanobubbles with a diameter of around 100 nm showed high stability and remained in water for a long time (Ushikubo *et al.*, 2010). Ohgaki *et al.* (2010) observed that 50 nm nitrogen, methane and argon nanobubbles lasted for more than 2 weeks.

During this study, ozone nanobubbles were measured at 10, 15, 20 and 25°C to determine the bubble behaviour, specifically the size and zeta potential of the bubbles, with temperature. The ozone nanobubbles were generated by operating the nanobubble generation system for 6 min with the generation chamber filled with 18 litres while keeping the temperature of the water constant. Within 20 min of bubble generation, 100 ml samples were tested for the bubble size and zeta potential. The observed bubble sizes are shown in Figure 4. The average size of the ozone nanobubbles varied between 100 and 200 nm. During analysis, it was observed that the average nanobubble diameter increased with increasing temperature.

The variation in zeta potential values with temperature is shown in Figure 5. The zeta potential values of the ozone nanobubbles decreased with increasing temperature. With an increase in temperature, ions in liquid gain energy, which increases their mobility within the liquid. Increased energy moves the high-energy ions away from the stern layer, reducing the thickness of the slipping plane, hence reducing the zeta potential. Jia *et al.* (2013) reported similar zeta potential values for air bubbles in water, where the bubble zeta potential decreased with an increase in temperature.

### Variation in ozone concentration with time

Elevated ozone concentrations in water increase the probability for ozone to react with chromium in sediments. The advantages of using ozone nanobubbles over using a diffuser (that generate macrobubbles (Figure 6(a))) to dissolve ozone in water was first tested. To compare the two methods, ozone was dissolved in water using ozone nanobubbles in one test and an air diffuser in the second test. The ozonation tank used during the test was filled to 20 litres with filtered tap water. Ozonation was performed for 3 min using the air diffuser by delivering ozone at a rate of 3 l/min at a pressure of 6·895 kPa. Ozonation using the nanobubble generator was run for 3 min by delivering ozone at the same rate and pressure. A sample of 800 ml was collected from both tests. Both samples were kept fully submerged in a constant-temperature water bath (Figure 6(b)) while keeping them

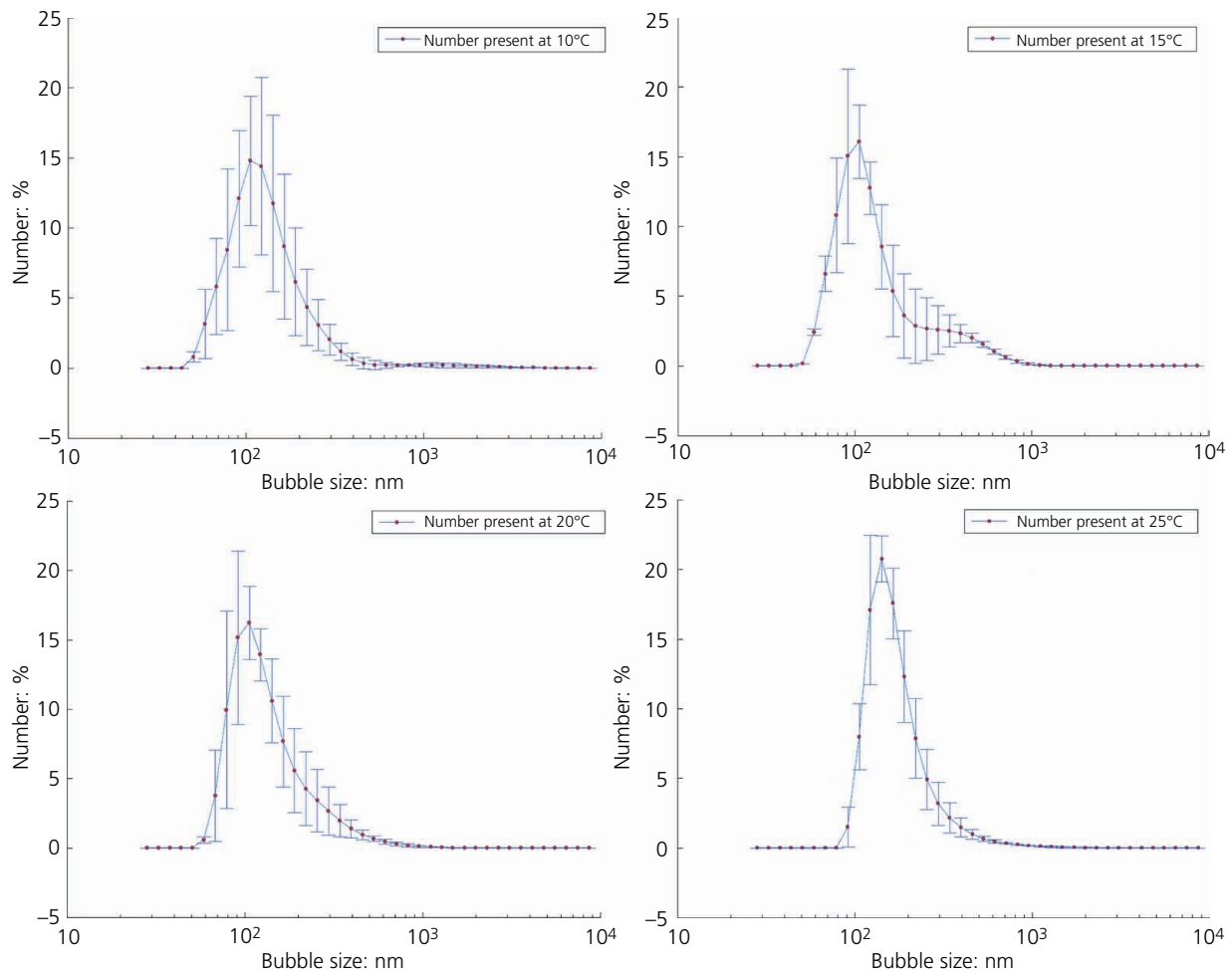


Figure 4. Ozone nanobubble size distribution at temperatures 10, 15, 20 and 25°C

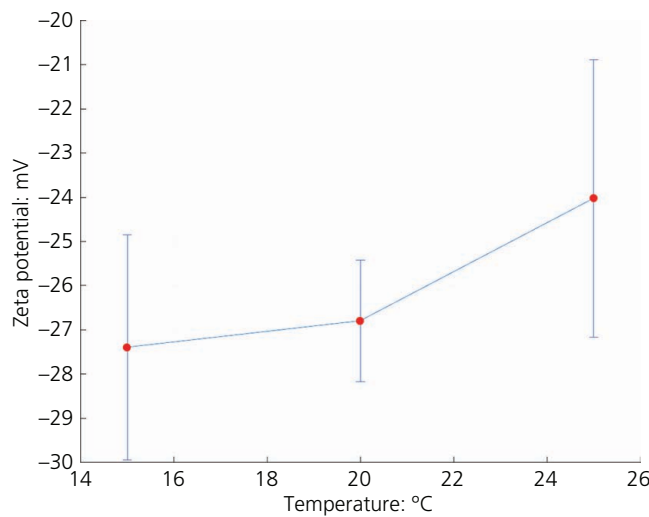


Figure 5. Zeta potential variation at temperatures of 15, 20 and 25°C

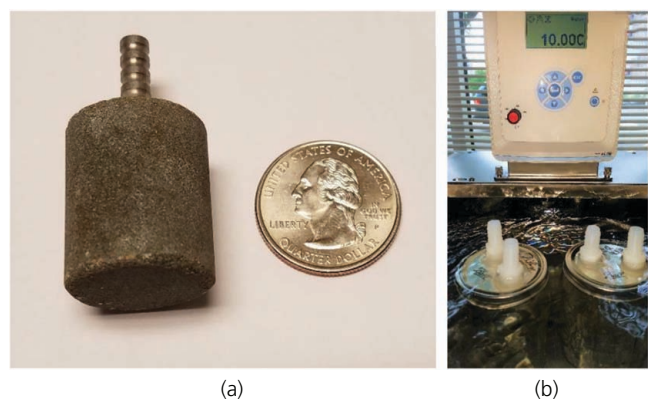


Figure 6. (a) Diffuser used in ozonation; (b) constant-temperature bath

ventilated to prevent any ozone build-up in the overhead space in the containers. Ozone and oxygen concentrations in the samples were measured for 8 h. Figure 7(a) shows the variation in ozone concentration with time at 20°C. Dissolved ozone concentrations in nanobubble-saturated water showed substantially elevated ozone concentrations compared to samples prepared with a regular air diffuser. Dissolved ozone concentrations obtained with nanobubbles reached a maximum value of 52.79 mg/l, while those using a conventional diffuser reached 39.39 mg/l.

The ozone concentration rapidly reduced when a regular air diffuser was used to dissolve ozone in water. With ozone nanobubbles, the amount of ozone after 1.6 h was equal to the initial ozone concentrations using a diffuser. The ozone concentration rapidly reduced during the first hour when a diffuser was used, whereas, with ozone nanobubbles, the ozone concentration rapidly reduced for 4 h and then both, ozone dissolved using a diffuser and ozone dissolved using nanobubbles gradually decreased. When a gas is bubbled, bubbles rise to the surface and burst. The smaller the bubble size, the longer the time that the bubble rises to the surface. Thus, the microbubbles generated from the diffuser steadily declined for over 1 h, while the nanobubbles steadily declined for over 4 h. The ozone nanobubbles concentration was above 10 mg/l for 7 h. Simultaneously, dissolved oxygen levels were also monitored. The dissolved oxygen levels in water at 20°C are shown in Figure 7(b). The highest oxygen levels were observed in water when a nanobubble generator was used to dissolve ozone in water. At 30 min, the oxygen concentration reached 37.28 mg/l, and then oxygen levels slowly decreased over time. However, compared to depletion of ozone, the rate of decline of oxygen was much slower due to the generation of oxygen due to decomposition of ozone.

#### Remediation of chromium-contaminated sediments

To determine optimum treatment levels for the removal of heavy metals, this study used a highly concentrated chromium-

contaminated soil to represent actual river sediments that contain multiple heavy metals. The high concentrations of chromium in the sample required long treatment durations.

The remediation of chromium-contaminated soil was performed in a chamber with 3 litre volume. The remediation chamber was first filled with ozone-nanobubble-saturated water, and then ultrasound was applied to the soil and water mixture while varying the ozone generation temperature, pH values, ultrasound power and dwell time. The impact of ultrasound on nanobubbles was investigated, and results showed that applying ultrasound for long durations was detrimental to remediation; specifically, a long duration of ultrasound treatment heated the water and hence reduced the dissolved gases and nanobubbles in water. Hence, to avoid such negative impact, ultrasound was applied in segments of 1–2 min during remediation. The removal efficiency of chromium was determined using the equation

$$1. \quad E = \frac{I - O}{I} \times 100$$

where  $I$  is the initial chromium concentration in the specimen and  $O$  is the chromium concentration at the end of the experiment. The initial chromium concentration of the samples was 3253 parts per million (ppm).

To test removal efficiency at different power levels, sonication was performed at 20°C and over 2 min intervals to prevent temperature increase followed by an average of 28 min to drain slowly the water from the reaction chamber. This process of sonication and draining was repeated for a total of 15 times. Figure 8 shows the test results. The lower power levels showed low removal efficiencies. A similar observation was also reported by Meegoda and Perera (2001) and Park and Son (2017).

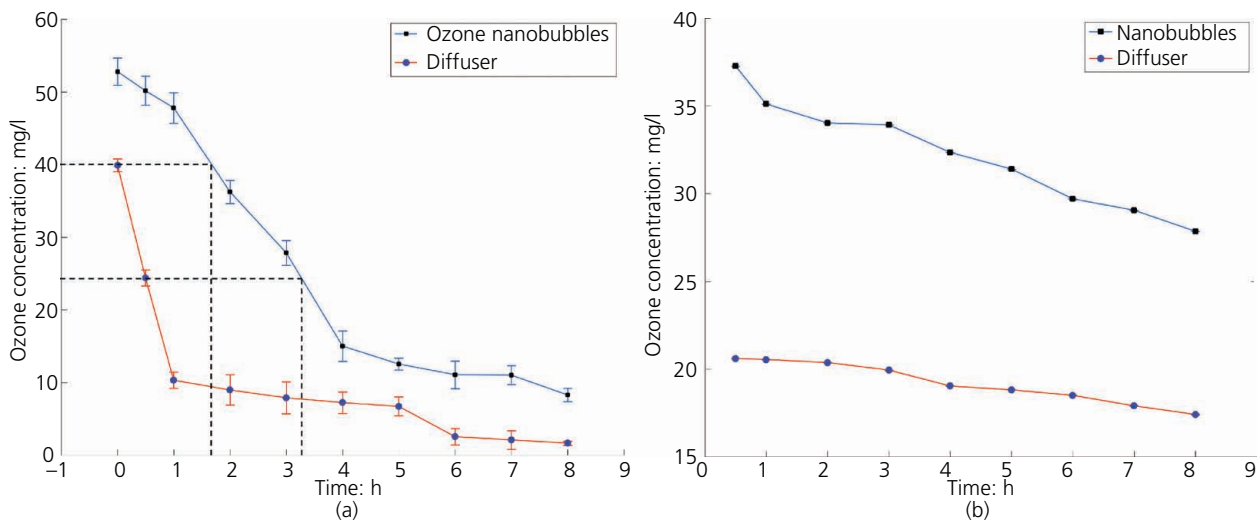


Figure 7. (a) Ozone concentration variation over time at 20°C; (b) dissolved oxygen variation over time at 20°C

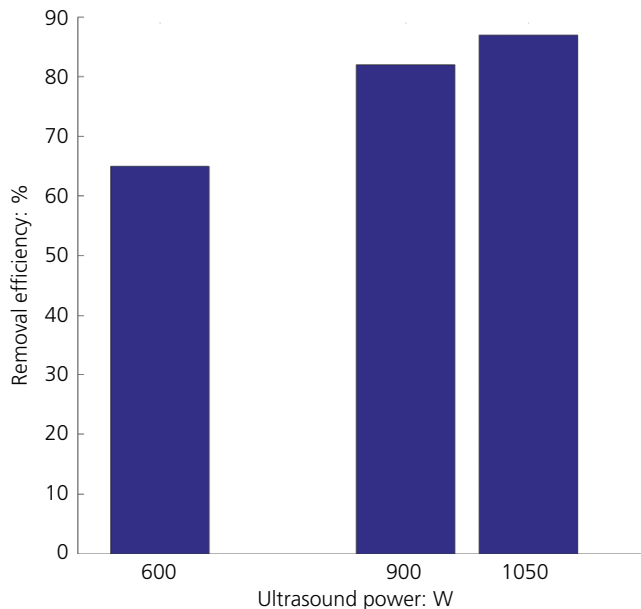


Figure 8. Sonication power and removal efficiency at 20°C

To test removal efficiency for different durations, the experiment was performed with ultrasound power kept at 1050 W, while the total sonication time was tested at 60 and 120 min where the sonication was applied at 2 min cycles, followed by an average of 28 min of draining. Figure 9 shows the test results. The removal efficiency of chromium reached 97.54% after 120 min of sonication with a total remediation time of 1800 min.

The pH value of water during remediation can significantly contribute to heavy metal removal. Park and Son (2017) showed high removal efficiencies at low pH values. This study evaluated

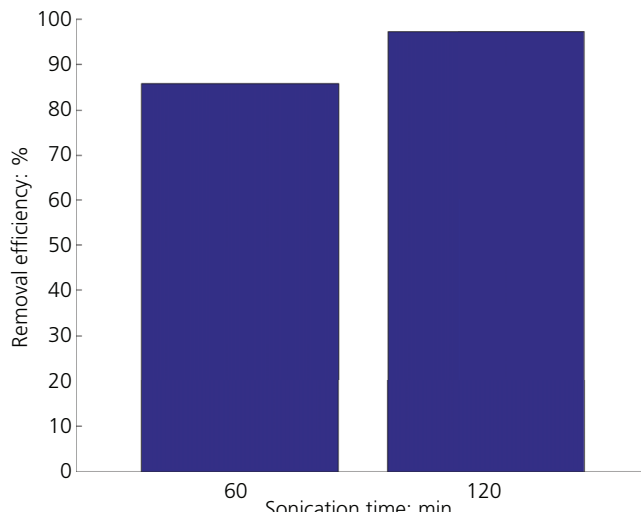


Figure 9. Chromium removal efficiency with time

the impact of pH on removal efficiency by testing at pH values of 4, 7 and 10. During the investigation, a soil sample was collected at the end of 10 min of total sonication. The experiments were performed by using 2 min sonication cycles. The initial chromium contamination level was tripled to 16.714 mg/g (16 714 ppm) in the synthetic contaminated soil for this test. Figure 10 shows the test results. The chromium concentration in the soil reduced over time for all pH levels, but the reduction rate was much higher at lower pH levels. Having a low pH level in water enhanced remediation, while remediation performed at high pH levels would not effectively remove chromium from the soil.

The chromium removal efficiency reached 99% for the solution with a pH value of 4. At a pH value of 10, the removal efficiency was low because chromium started to precipitate by creating chromium (III) hydroxide ( $\text{Cr(OH)}_3$ ), which is not water soluble. Chromium in an alkaline environment tends to precipitate, making it difficult to separate chromium from soil. Hence, creating an acidic environment for the removal of chromium will increase the removal efficiency.

To observe chromium adsorption onto soil particles visually, a scanning electron microscope (SEM) was used to identify the impact of ozone nanobubbles and ultrasound on the soil. The SEM image captured before remediation of soil is shown in Figure 11(a). A Leo 1530VP-Zyvex nanomanipulator system/cryosystem SEM was used for imaging.

Results from SEM images showed chromium deposits on the soil particles. The deposits surround the soil particles, creating adsorption bonds. Remediation of these sediments breaks the adsorption bonds and oxidises chromium. SEM imaging was performed on partially remediated sediments after 15 min of total

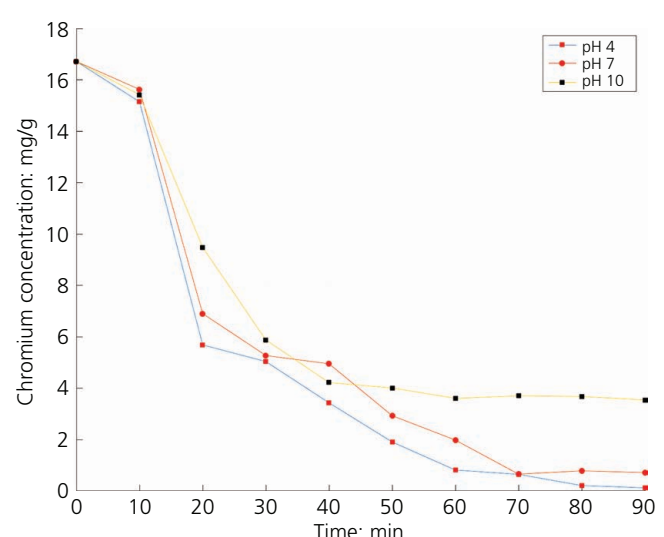


Figure 10. Chromium concentration with time (pH 4, pH 7 and pH 10)

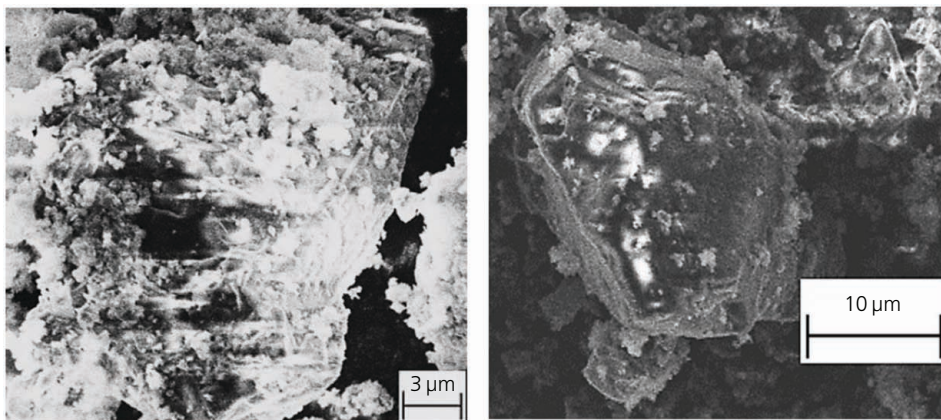


Figure 11. SEM imaging: (a) chromium-contaminated soil; (b) soil after 14 min of treatment

sonication. The image obtained of remediated sediments after 15 min of total sonication is shown in Figure 11(b).

## Summary and conclusions

This research investigated the use of ultrasound and ozone nanobubbles to remove chromium from contaminated sediments, testing efficiency and effectiveness at varying power, pH and duration. Increasing the ultrasound power improved the remediation. Changing the pH of the solution changed the chromium removal efficiency. At higher solution pH values, the chromium removal efficiency decreased, whereas low pH values showed faster and higher removal rates. At longer durations, chromium removal efficiency increased. The final removal efficiencies reached 97.54% when the experiment was performed for 120 min of sonication with pH of 7 and power level of 1050 W.

Ozone nanobubbles increased the solubility of ozone in water and reduced wastage. Due to the high ozone concentrations in water, chromium oxidation increased. When nanobubbles are used as a delivery method, a reduced amount of ozone was required to oxidise chromium, saving money and reducing the impact on the environment from released ozone gas during treatment.

The laboratory-scale experiments showed convincing results of decontaminating heavy-metal-contaminated soil with ultrasound and ozone nanobubbles. Future pilot-scale studies are proposed to refine the technology for field application and cost-benefit analysis.

## Acknowledgement

This research was sponsored by US National Science Foundation Award Number 1634857, entitled 'Remediation of Contaminated Sediments with Ultrasound and Ozone Nano-bubbles'.

## REFERENCES

Babić S, Petrović M and Kaštelan-Macan M (1998) Ultrasonic solvent extraction of pesticides from soil. *Journal of Chromatography A* **823**(1): 3–9, [https://doi.org/10.1016/S0021-9673\(98\)00301-X](https://doi.org/10.1016/S0021-9673(98)00301-X).

Bagal MV and Gogate PR (2012) Sonochemical degradation of alachlor in the presence of process intensifying additives. *Separation and Purification Technology* **90**: 92–100, <https://doi.org/10.1016/j.seppur.2012.02.019>.

Brenner MP and Lohse D (2008) Dynamic equilibrium mechanism for surface nanobubble stabilization. *Physical Review Letters* **101**(21): 214505, <https://doi.org/10.1103/PhysRevLett.101.214505>.

Bunkin NF, Yurchenko SO, Suyazov NV and Shkirin AV (2012) Structure of the nanobubble clusters of dissolved air in liquid media. *Journal of Biological Physics* **38**(1): 121–152, <https://doi.org/10.1007/s10867-011-9242-8>.

Choi H, Kim YY, Lim H et al. (2001) Oxidation of polycyclic aromatic hydrocarbons by ozone in the presence of sand. *Water Science & Technology* **43**(5): 349–356, <https://doi.org/10.2166/wst.2001.0323>.

Do SH, Jo JH, Jo YH, Lee HK and Kong SH (2009) Application of a peroxyomonosulfate/cobalt (PMS/Co(II)) system to treat diesel-contaminated soil. *Chemosphere* **77**(8): 1127–1131, <https://doi.org/10.1016/j.chemosphere.2009.08.061>.

Feng H, Onwueme V, Jaslanek WJ, Stern EA and Jones KW (2004) Lower Passaic River sediment pollution study using GIS, New Jersey, USA. *Proceedings of International Conference on Urban Dimensions of Environmental Change: Science, Exposures, Policies and Technologies, Shanghai, China*, pp. 275–282.

Hampton MA and Nguyen AV (2010) Nanobubbles and the nanobubble bridging capillary force. *Advances in Colloid and Interface Science* **154**(1): 30–55, <https://doi.org/10.1016/j.cis.2010.01.006>.

Ikeura H, Kobayashi F and Tamak M (2011) Removal of residual pesticides in vegetables using ozone microbubbles. *Journal of Hazardous Materials* **186**(1): 956–959, <https://doi.org/10.1016/j.jhazmat.2010.11.094>.

Jia W, Ren S and Hu B (2013) Effect of water chemistry on zeta potential of air bubbles. *International Journal of Electrochemical Science* **8**: 5828–5837.

Jin F, Ye J, Hong L, Lam H and Wu C (2007) Slow relaxation mode in mixtures of water and organic molecules: supramolecular structures or nanobubbles? *Journal of Physical Chemistry B* **111**(9): 2255–2261, <https://doi.org/10.1021/jp068665w>.

Khuntia S, Kumar SM and Ghosh P (2013) Removal of ammonia from water by ozone microbubbles. *Industrial & Engineering Chemistry Research* **52**: 318–326, <https://doi.org/10.1021/ie302212p>.

Kylloinen, H, Pirkonen P, Hintikka V et al. (2004) Ultrasonically aided mineral processing technique for remediation of soil contaminated by heavy metals. *Ultrasonics Sonochemistry* **11**(3–4): 211–216, <https://doi.org/10.1016/j.ultsonch.2004.01.024>.

Leštan D and Finžgar N (2007) Leaching of Pb contaminated soil using ozone/UV treatment of 669 EDTA extractants. *Separation Science and Technology* **42**(10): 2133–2140, <https://doi.org/10.1080/08824200701250001>.

Technology **42**: 1575–1584, <https://doi.org/10.1016/j.chemosphere>. 2005.09.015.

Li P, Tsuge H and Itoh K (2009) Oxidation of dimethyl sulfoxide in aqueous solution using microbubbles. *Industrial & Engineering Chemistry Research* **48**(17): 8048–8053, <https://doi.org/10.1021/ie801565v>.

Li D, Jing D, Pan Y, Wang W and Zhao X (2014) Coalescence and stability analysis of surface nanobubbles on the polystyrene/water interface. *Langmuir* **30**(21): 6079–6088, <https://doi.org/10.1021/la501262a>.

Li D, Jing D, Pan Y, Bhushan B and Zhao X (2016) Study of the relationship between boundary slip and nanobubbles on a smooth hydrophobic surface. *Langmuir* **32**(43): 11287–11294, <https://doi.org/10.1021/acs.langmuir.6b02877>.

Masten, SJ and Davies SHR (1997) Efficacy of in-situ for the remediation of PAH contaminated soils. *Journal of Contaminant Hydrology* **28**(4): 327–335, [http://doi.org/10.1016/S0169-7722\(97\)00019-3](http://doi.org/10.1016/S0169-7722(97)00019-3).

Meegoda JN and Perera R (2001) Ultrasound to decontaminate heavy metals in dredged sediments. *Journal of Hazardous Materials* **85**(1): 73–89, [https://doi.org/10.1016/S0304-3894\(01\)00222-9](https://doi.org/10.1016/S0304-3894(01)00222-9).

Meegoda JN and Veerawat K (2002) Ultrasound to decontaminate organic compounds in dredged sediments. *Soil and Sediment Contamination* **11**(1): 91–116, <https://doi.org/10.1080/20025891106718>.

Meegoda JN, Batagoda JH and Aluthgun-Hewage S (2017) Briefing: In situ decontamination of sediments using ozone nanobubbles and ultrasound. *Journal of Environmental Engineering and Science* **12**(1): 1–3, <https://doi.org/10.1680/jenes.17.00006>.

Modi KK, Jana A, Ghosh S, Watson R and Pahan K (2014) A physically-modified saline suppresses neuronal apoptosis, attenuates tau phosphorylation and protects memory in an animal model of Alzheimer's disease. *PLoS ONE* **9**(8): e103606, <https://doi.org/10.1371/journal.pone.0103606>.

Mondal S, Martinson JA, Ghosh S, Watson R and Pahan K (2012) Protection of Tregs, suppression of Th1 and Th17 cells, and amelioration of experimental allergic encephalomyelitis by a physically-modified saline. *PLoS ONE* **7**(12): e51869.

Newman AP, Lorimer JP, Mason TJ and Hunt KR (1997) An investigation into the ultrasonic treatment of polluted solids. *Ultrasonics Sonochemistry* **4**(2): 153–156, [https://doi.org/10.1016/S1350-4177\(97\)00020-5](https://doi.org/10.1016/S1350-4177(97)00020-5).

O'Mahony MM, Dobson ADW, Barnes JD and Singleton I (2006) The use of ozone in the remediation of polycyclic aromatic hydrocarbon contaminated soil. *Chemosphere* **63**(2): 307–314, <https://doi.org/10.1016/j.chemosphere.2005.07.018>.

Ohgaki K, Khanh NQ, Joden Y, Tsuji A and Nakagawa T (2010) Physicochemical approach to nanobubble solutions. *Chemical Engineering Science* **65**(3): 1296–1300, <https://doi.org/10.1016/j.ces.2009.10.003>.

Pan G and Yang B (2012) Effect of surface hydrophobicity on the formation and stability of oxygen nanobubbles. *ChemPhysChem* **13**(8): 2205–2212, <https://doi.org/10.1002/cphc.201100714>.

Park B and Son Y (2017) Ultrasonic and mechanical soil washing processes for the removal of heavy metals from soils. *Ultrasonics Sonochemistry* **35**: 640–645, <https://doi.org/10.1016/j.ulsonch.2016.02.002>.

Rice EW, Baird RD, Eaton AD and Clesceri LS (eds) (2017) *Standard Methods for Water and Wastewater Examination*, 22nd edn. American Public Health Association, American Water Works Association and Water Environment Federation, Washington, DC, USA.

Rodman DL, Carrington NA and Xue ZL (2006) Conversion of chromium (III) propionate to chromium (VI) by the advanced oxidation process: pretreatment of a biomimetic complex for metal analysis. *Talanta* **70**(3): 668–675, <https://doi.org/10.1016/j.talanta.2006.05.092>.

Sedlák M (2006a) Large-scale supramolecular structure in solutions of low molar mass compounds and mixtures of liquids: I. light scattering characterization. *Journal of Physical Chemistry B* **110**(9): 4329–4338, <https://doi.org/10.1021/jp0569335>.

Sedlák M (2006b) Large-scale supramolecular structure in solutions of low molar mass compounds and mixtures of liquids: II. kinetics of the formation and long-time stability. *Journal of Physical Chemistry B* **110**(9): 4339–4345, <https://doi.org/10.1021/jp056934x>.

Seo SH, Sung BW, Kim GJ et al. (2010) Removal of heavy metals in an abandoned mine drainage via ozone oxidation: a pilot-scale operation. *Water Science & Technology* **62**(9): 2115–2120, <https://doi.org/10.2166/wst.2010.406>.

Takahashi M (2009) Base and technological application of micro-bubble and nano-bubble. *Materials Integration* **22**: 2–19.

Urban JD, Tachovsky JA, Haws LC, Wikoff Staskal D and Harris MA (2009) Assessment of human health risks posed by consumption of fish from the Lower Passaic River, New Jersey. *Science of the Total Environment* **408**(2): 209–224, <https://doi.org/10.1016/j.scitotenv.2009.03.004>.

USACE (US Army Corps of Engineers) (1973) *Maintenance of the Newark Bay, Hackensack, and Passaic Rivers Navigation Project, New Jersey: Final Environmental Statement*. USACE New York District, New York, NY, USA.

Ushikubo FY, Furukawa T, Nakagawa R et al. (2010) Evidence of the existence and the stability of nano-bubbles in water. *Colloids and Surfaces A: Physicochemical and Engineering Aspects* **361**(1): 31–37, <https://doi.org/10.1016/j.colsurfa.2010.03.005>.

Wang Y, Bhushan B and Zhao X (2009) Improved nanobubble immobility induced by surface structures on hydrophobic surfaces. *Langmuir* **25**(16): 9328–9336, <https://doi.org/10.1021/la901186a>.

Yu DY, Kang N, Bae W and Banks MK (2007) Characteristics in oxidative degradation by ozone for saturated hydrocarbons in soil contaminated with diesel fuel. *Chemosphere* **66**(5): 799–807, <https://doi.org/10.1016/j.chemosphere.2006.06.053>.

## How can you contribute?

To discuss this paper, please submit up to 500 words to the editor at [journals@ice.org.uk](mailto:journals@ice.org.uk). Your contribution will be forwarded to the author(s) for a reply and, if considered appropriate by the editorial board, it will be published as a discussion in a future issue of the journal.